Published in final edited form as:
J Magn Reson Imaging. 2012 May ; 35(5): 1026–1037. doi:10.1002/jmri.23581.

Applications of Arterial Spin Labeled MRI in the Brain

John A. Detre, MD[1,2,3], **Hengyi Rao, PhD**[1,3], **Danny JJ Wang**[4], **Yu Fen Chen, PhD**[5], and **Ze Wang, PhD**[3,6]

[1]Department of Neurology, University of Pennsylvania

[2]Department of Radiology, University of Pennsylvania

[3]Center for Functional Neuroimaging, University of Pennsylvania

[4]Department of Neurology, UCLA

[5]Department of Radiology, Northwestern University

[6]Department of Psychiatry, University of Pennsylvania

Abstract

Perfusion provides oxygen and nutrients to tissues and is closely tied to tissue function, and disorders of perfusion are major sources of medical morbidity and mortality. It has been almost two decades since the use of arterial spin labeling (ASL) for noninvasive perfusion imaging was first reported. While initial ASL MRI studies focused primarily on technological development and validation, a number of robust ASL implementations have emerged, and ASL MRI is now also available commercially on several platforms. As a result, basic science and clinical applications of ASL MRI have begun to proliferate. Although ASL MRI can be carried out in any organ, most studies to date have focused on the brain. This review covers selected research and clinical applications of ASL MRI in the brain to illustrate is potential in both neuroscience research and clinical care.

Keywords

arterial spin labeling; cerebral blood flow; brain function; cognitive neuroscience; clinical neuroscience; magnetic resonance imaging

Introduction

Tissue perfusion is a fundamental physiological parameter that is closely linked to tissue function, and disorders of perfusion are leading causes of medical morbidity and mortality. While a number of flow-related parameters can be measured using a range of MRI methodologies, direct measurement of tissue perfusion in classical units of ml/g/min requires a nominally diffusible tracer. This was first accomplished in MRI using deuterated water (1,2) and fluorinated (3,4) tracers, and in the future hyperpolarized tracers may be used, but currently the most effective approach uses magnetically labeled arterial blood water, termed “arterial spin labeling” (ASL). Feasibility of the basic ASL approach for imaging tissue perfusion was first published in 1992 as a crude single-slice image in the rat brain (5). Since that time there have been several important methodological advances and

Corresponding Author: John A. Detre, MD, Professor, Depts. of Neurology and Radiology, Director, Center for Functional Neuroimaging, School of Medicine, University of Pennsylvania, 3 W. Gates Bldg./HUP, 3400 Spruce St., Philadelphia, PA 19104-4283, 215-573-8487 (office), FAX: 215-349-8260, detre@mail.med.upenn.edu.

technical improvements, such that it is currently possible to obtain whole-brain ASL data routinely in both clinical and research settings. With the maturation of this technology, numerous basic and clinical applications have also been assessed. The majority of initial applications have been in the brain due to its high perfusion rates relative to other organs, its spatially consolidated blood supply, the lack of major motion issues, and the normally tight coupling between regional cerebral blood flow and neural activity.

This review primarily focuses on applications of ASL, though a brief introduction to ASL methodologies is also provided as background. There are currently approximately one thousand articles on ASL MRI and its applications. Accordingly, this review is not intended to provide a comprehensive summary of the literature. Instead, it attempts to illustrate the particular benefits of ASL MRI in selected applications in basic and clinical neuroscience where it has shown promise.

ASL Methodology

In ASL techniques, arterial blood water is magnetically "labeled" using radiofrequency (RF) irradiation. The approach is highly analogous to PET CBF measurements, which use ^{15}O labeled water as the flow tracer, except that the magnetically labeled arterial water "decays" with T1 relaxation rather than the radioactive decay rate for ^{15}O. ASL MRI measurements of cerebral blood flow have been validated against ^{15}O-PET (6–8) in the brain and have been shown to provide similar image appearance and blood flow values. Because the T1 relaxation rate for water in blood or tissues is on the order of 1–2 seconds, only small amounts of arterial spin labeled water accumulate in the brain, and prolongation of T1 with field strength represents a major benefit of high-field MRI for ASL studies. Fortunately, 3 Tesla MRI machines are now widespread. Signal gains of up to four-fold are theoretically obtainable from 7 Tesla ASL, but there are also numerous challenges to realizing this benefit.

A consequence of the short lifetime of the magnetic label is that perfusion measurements are very sensitive to the arterial transit times of the label (9). Uncertainties in the arterial transit time are the major source of error in most ASL studies, and it can be challenging to measure blood flow in poorly perfused tissues due to label decay during transit. Use of a post-labeling delay to reduce the transit time dependence of ASL was an early advance in the methodology (9), and is now routinely employed in many ASL implementations. On the other hand, arterial transit times derived from ASL data are potentially informative by defining vascular and watershed territories (10–12) or collateral flow sources (13,14).

During ASL image acquisition, repeated label and control images are typically interleaved. Perfusion contrast is obtained by pair-wise subtraction of the label and control acquisitions, and absolute CBF in well-characterized physiological units of ml/100g/min can be estimated by modeling expected signal changes in the brain, primarily taking into account the tracer half-life determined by the T1 of blood and tissue (5). During the past two decades, theoretical and experimental studies have been conducted to improve the accuracy of CBF quantification using ASL by taking into account multiple parameters such as arterial transit time, magnetization transfer effect, T1, labeling efficiency, and capillary water permeability. Assumed values are typically used for these parameters since it can be time-consuming to measure them in each subject and using measured values adds noise to the resulting CBF maps. Variations in labeling efficiency, arterial transit time, and blood T1 are the most significant sources of error in CBF quantification (15), particularly in clinical applications where major deviations from normative values occur. While many ASL quantification schemes are based on a steady-state model derived from diffusible tracer theory, kinetic models analogous to those used for dynamic susceptibility contrast perfusion MRI have also

been applied to ASL data (16,17), and are theoretically insensitive to variations in parameters such as arterial transit time and labeling efficiency. Better characterization of the compartmentalization of the arterial spin label and the use of advanced signal processing schemes to improve ASL quantification remain promising avenues for improving its sensitivity and reliability (18). Although reliable quantification of absolute CBF based on ASL data remains challenging, similar challenges and assumptions exist for other methods for quantifying CBF in vivo.

Several approaches exist for achieving ASL (Figure 1). In continuous ASL (CASL) arterial blood water is continuously and selectively labeled as it passes through a labeling plane (19). In pulsed ASL (PASL) a short RF pulse is used to instantaneously invert blood and tissue, and can be applied either below the brain (20,21), or to the entire brain with subsequent selective inversion of the imaging slices to produce a magnetization difference between blood and brain water (22). A hybrid approach that simulates CASL using many short pulses termed “pseudocontinuous” or “pulsed continuous” ASL (pCASL) combines these schemes to provide better sensitivity and ease of implementation for body coil transmitters (23,24). Several methods also exist for spatially selective labeling, uniquely allowing the perfusion distribution of single arterial territories to be measured (25–30). Velocity selective labeling has also been explored as a means of eliminating arterial transit time dependence (31,32). More recently time-resolved ASL has been developed as a noninvasive alternative to angiography (33).

Any imaging sequence can be used to measure the changes in tissue magnetization due to ASL. Since the ASL effect is small, it is desirable to use an imaging sequence with high SNR. Much of the data acquired to date using ASL has employed echoplanar imaging due to its high SNR and speed, which reduces the potential for motion artifacts between label and control scans. However, echoplanar imaging can introduce distortions in regions of high static susceptibility gradients that degrade image quality. Over the past several years, 3D sequences based on fast spin echo (24) or GRASE (34) have begun to be used for image acquisition in ASL to improve image quality. 3D sequences provide improved SNR and greatly facilitate the use of background suppression pulses to reduce the static brain signal to increase sensitivity (35–37).

Clinical applications of ASL

Commercial ASL sequences are now available for most major clinical MRI platforms. These vary considerably with regard to the specific implementation used for labeling, imaging, and quantification, but they do allow ASL to be added to clinical imaging protocols. As with many other MRI methodologies, this has initially been most widely applied in the brain.

An obvious application of ASL MRI is in cerebrovascular disease since it is a disorder of perfusion (Figure 2). A few early studies demonstrated that ASL MRI was feasible in acute stroke (38,39), but the lack of availability of robust methodology, its low sensitivity for hypoperfusion, and the requirement for several minutes of signal averaging limited its use, so to date DSC perfusion MRI remains the predominant method in use for acute stroke. However, the use of background suppression allows ASL MRI data to be reliably obtained at 3T in less than one minute (36), and as this methodology becomes available, the use of ASL MRI in acute stroke imaging protocols may increase. Nonetheless, several case reports demonstrate the utility of ASL in stroke and its differential diagnosis, with unexpected hyperperfusion suggesting stroke mimics such as complicated migraine (40) and focal seizure (41).

While acute stroke has been the focus of much of cerebrovascular MRI, the capability for accurate and reliable quantification of cerebral blood flow (CBF) with ASL provides as-yet

untapped potential applications in managing chronic cerebrovascular disease. Early data demonstrated that CBF is chronically reduced in patients with cerebrovascular disease, and ASL MRI could play an important role in monitoring CBF with medical and surgical management changes (42–45). Vessel selective ASL may also have a role in planning and monitoring interventional procedures (46). ASL MRI can also be used in the diagnosis and management of arteriovenous malformations to increase their conspicuity of due to the accumulation of a large venous label, and potentially to quantify shunt fractions (47).

ASL MRI is appealing in pediatric populations due to its noninvasiveness. It has been used to assess brain tissue perfusion in children with sickle cell disease showing a significant increase of CBF in all cerebral arterial territories, which concurred with previous PET findings (48), in acute stroke where ASL perfusion deficits predicted chronic infarct volumes while normally or hyperperfused vascular territories were generally associated with positive imaging outcomes (49), and in congenital heart disease where baseline CBF was found to be reduced and periventricular leukomalacia was associated with low CBF and lack of flow response to hypercarbia (50).

Arterial occlusive disease is not limited to the brain, but because the brain is stationary and highly perfused, it is easier to obtain good quality ASL data in brain than in other organs. However, ASL MRI has also been obtained from post-ischemic extremities in patients with peripheral vascular disease (51) and there have been some preliminary feasibility studies of ASL MRI in the heart (52). The kidneys and retina are highly perfusion tissues where ASL MRI has also been used (53,54).

Another clinical area in which tissue perfusion represents a key pathophysiological mechanism is neoplastic disease and its treatment. Tumor vascularization and perfusion tends to increase with tumor grade, and brain tumor blood flow measured by ASL MRI has been shown to correlated with grade (55,56). Imaging tumor blood flow and metabolism can also be used to differentiate tumor recurrence from radiation necrosis (57) and to monitor treatment. Finally, treatment of neoplastic disease with antiangiogenesis therapy specifically targets the mechanisms by which tumors increase their vascularization, and preliminary studies demonstrate that early treatment responses detected by ASL MRI are predictive of subsequent clinical responses (58).

In brain and in most other organs, changes in perfusion are coupled to changes in metabolism. This provides the physiological basis of functional MRI studies, which will be discussed below, but also has clinical relevance. Several studies have supported the utility of ASL MRI for detecting patterns of regional hypoperfusion suggesting a diagnosis of Alzheimer's dementia (59–63) or frontotemporal dementia (61,63). Although a growing number of molecular imaging tracers are likely to provide the earliest and most specific detection of Alzheimer's neuropathology, there remains a role for functional imaging in predicting disease conversion (64) and monitoring disease progression and perhaps responses to therapy. Furthermore, molecular imaging studies are costly and not widely available, so there might also be an important role for ASL MRI in screening for neurodegenerative disease.

Epilepsy is another neurological disorder in which functional imaging contributes to diagnosis and management. Interictal hypoperfusion measured by ASL MRI has been shown to correlate with interictal hypometabolism by FDG-PET in temporal lobe epilepsy in a few preliminary studies (65–67), some showing correlations with PET data, and ictal hyperperfusion has also been visualized (41,68).

Basic Science Applications of ASL MRI

ASL MRI is a particularly promising MRI methodology for basic research because it is quantitative and because it is one of the few MRI contrast mechanisms for which the biological basis is well understood. Over the past decade, ASL MRI has been successfully used in a variety of research applications, mainly in the neuroscience, and it is now increasingly included in multimodal neuroimaging protocols. Here we review several of the research areas in which ASL MRI has been assessed. ASL MRI has also been used to further investigate changes in blood oxygenation level dependent (BOLD) contrast, which represents a complex interaction between changes in blood flow, blood volume, and oxygen metabolism. One such application is "calibrated BOLD" (69), wherein relative changes in ASL CBF and BOLD contrast with vasoactive stimuli are used to draw inferences about oxygen metabolism changes with functional stimulation.

ASL for developmental neuroscience

ASL MRI is currently being used as a biomarker for functional brain development in both healthy populations and developmental disorders (Figure 3). Several physiological properties of the pediatric brain are beneficial for ASL (70). Blood flow rates are generally higher in children compared to adults (except in newborns) (71), which increases perfusion contrast, and the water content of the brain is also higher in children than adults, which yields a greater concentration and half-life of the tracer (blood water). In addition, ASL offers quantitative cerebral blood flow (CBF) at baseline without the use of external tasks, which is more convenient and advantageous than performing task activation fMRI in infants and younger children.

The first feasibility study of pediatric ASL was carried out using pulsed ASL (PASL) at 1.5T (70), which demonstrated a 70% improvement in the SNR of pediatric perfusion images as compared to those of healthy adults. Several recent studies have more systematically investigated developmental changes of brain perfusion, using pulsed or continuous ASL (CASL) at 1.5 and 3T (72–75). In healthy children older than 4 to 5 years, a trend of decreasing CBF in the whole brain, gray and white matter with age has been observed (73,74), which is in agreement with existing literature based on nuclear medicine approaches (SPECT) (71). In terms of developmental trajectories of regional CBF (rCBF), relative rCBF increases with age (after adjusting global CBF) were observed in the frontal cortex, cingulate cortex, angular gyrus, and hippocampus (74), which may reflect the later maturation of cortical regions associated with executive function, cognitive control, integrative and memory function (76). In a recent study performed on 202 healthy children aged 5–18 years (75), Taki et al. separated developmental effects on brain structure and perfusion by calculating brain perfusion with adjustment for gray matter density (BP-GMD) in 22 brain regions. The correlation between BP-GMD and age showed an inverted U shape followed by a U-shaped trajectory in most regions. The age at which BP-GMD peaked increased from the occipital to the frontal lobe via the temporal and parietal lobes.

ASL MRI has also been applied to neonates and infants. In unsedated newborns, cortical perfusion level is lower than that of adults. Nevertheless, perfusion is significantly higher in basal ganglia than cortical gray and white matter (72), consistent with PET imaging results in this age group (77). Another recent study compared perfusion images acquired from normally developing 7- and 13-month-old infants while asleep without sedation (78). The 13-month infant group showed an increase of relative CBF in frontal regions as well as in the hippocampi, anterior cingulate, amygdalae, occipital lobes, and auditory cortex.

ASL for Cognitive Neuroscience

Over the last two decades, functional MRI (fMRI) based on BOLD has become a standard tool to visualize regional brain activation in response to various sensorimotor or cognitive tasks. However, because BOLD signal is the result of a complex interaction between a number of physiological variables changes accompanying neural activity including CBF, cerebral blood volume (CBV), and cerebral oxygenation metabolic rate, task-specific BOLD signal changes cannot be directly quantified in physiological units. Instead, BOLD signal changes are usually expressed as a relative percentage signal change or as a statistical significance level based on a statistical model. ASL perfusion MRI can be used to monitor task correlated CBF changes in a manner similar to BOLD fMRI. Although task correlated percentage signal changes in ASL MRI are weaker than BOLD changes, there is evidence that ASL CBF changes are better localized than BOLD changes both spatially (79) and temporally (80,81). However, these benefits have yet to be realized in significant applications. Instead, the principal benefits of ASL MRI for brain mapping relate to the quantitative relationship between ASL MRI signal changes and CBF.

ASL data are typically obtained from successive pairwise subtractions between images acquired with and without arterial spin labeling. This paired subtraction dramatically changes the noise properties of ASL compared with BOLD fMRI by eliminating low-frequency noise (82), thereby increasing sensitivity over longer time scales (83). The superior low-frequency sensitivity of ASL perfusion over BOLD fMRI has been well demonstrated in a sensorimotor study showing that reliable CBF activation in motor cortex could be detected with up to 24 hours interval between rest and finger tapping while BOLD activation diminished with a few minutes interval (84), as shown in Figure 4. Because of its long-term stability, ASL perfusion fMRI provides an appealing alternative to BOLD fMRI for imaging brain activations during long time scale processes and more ecological paradigms such as motor learning (85), emotion or mental states (86–88), mood changes (89,90), and natural vision (91). Further, although the sensitivity and temporal resolution of ASL are generally lower than routine BOLD fMRI, there is some evidence that ASL sensitivity to group effects is increased, which may be due to reduced between-subject variation in the CBF changes as compared to BOLD signal changes (83,84).

Because ASL MRI provides absolute quantification of CBF, which is coupled to regional neural activity (84), it can also be used to measure resting brain function independent of any specific sensorimotor or cognitive task. Indeed, it is thought that the vast majority of brain metabolism does not vary with exogenous stimuli, but rather reflects “state” or “trait” functions (92), which can be measured with ASL MRI. Using a latent trait-state model on ASL CBF data obtained over several weeks with eyes open or eyes closed, a recent study confirmed that approximately 70% of the CBF variance was attributable to individual differences on a latent physiological trait, with approximately 20% attributable to ‘state’ effects and the remaining variance attributable to measurement errors (93).

Several recent reports have begun to use ASL MRI to demonstrate genotype and phenotype “trait” effects (Figure 5). For example, ASL perfusion fMRI has been used to examine the effect of 5-HTTLPR (serotonin transporter) genetic variations on resting brain function and mood regulation of healthy individuals (89,94,95). The results showed that the homozygous short allele (s/s) group has increased resting CBF in the amygdala compared with the homozygous long allele (l/l) group, which could not be accounted for by variations in brain anatomy, personality, or self-reported mood (94). Moreover, regional CBF in the amygdala showed positive correlations with depression scores and stressful life events in the s/s group but negative correlations in the l/l group (95,96). These findings complement existing literature on short allele related amygdala hyperactivity and suggest an additional

neurobiological mechanism whereby the 5-HTTLPR is associated with individual differences in vulnerability to mood disorder. Other groups have also showed that resting baseline CBF correlates with habitual emotion regulation scores (97), working memory capacity (98), and predicts individual differences in the blood pressure response to a stress-eliciting task administered after MRI (99). Taken together, these studies indicate the potential of ASL perfusion fMRI for imaging the neural correlates of behavioral traits or states, and as such can be considered complementary to BOLD fMRI studies that focus more on evoked responses.

The ability to measure static brain function also proves an alternative approach to elucidating brain-behavior relationships to task activation by correlating regional CBF measures in the absence of a specific cognitive task with measures in other domains made outside of the MRI scanner. This approach relies on individual difference across the study cohort to provide image contrast, and its most effective use requires quantitative neuroimaging measures that can be effectively compared across subjects and scanning sessions. To date, this approach has mainly been used with structural MRI and termed "voxel based morphometry (VBM)" (100), but it can equally be applied to brain function using ASL MRI. This strategy of deriving brain-behavior relationships avoids the performance confound that is inherent in task activation data, which can be particularly problematic when studying populations with performance deficits.

ASL MRI as a Biomarker of Pharmacological Actions

Pharmacological imaging offers in-vivo visualization of drug actions and can be applied in both preclinical models and human subjects. The most widely applied pharmacological imaging method to date has been positron emission tomography (PET), which allows the distribution of radiotracer analogs of drugs or drug targets to be imaged. While this provides a very specific biomarker for drug penetrance and actions, it requires expensive development for each compound as well as exposure to ionizing radiation. Nonspecific PET markers of neural activity such as 15O-PET and FDG-PET have also been used, and more recently pharmacological MRI (phMRI) has begun been used for this purpose. These nonspecific approaches rely on a coupling between drug actions on neural activity and changes in CBF and metabolism. PhMRI based on BOLD contrast has been the most commonly used phMRI technique, but since BOLD does not provide a quantitative baseline it is primarily applicable to studying short term effects of intravenously administered drugs or drug effects on task-induced activations The complex interplay of physiological properties that give rise to BOLD contrast can also make interpretation difficult, especially when examining the effects of drugs that modulate both neural activity and blood flow.

One such substance is caffeine, a nonspecific adenosine antagonist that has the dual effect of decreasing CBF and increasing neural activity. Depending on the balance between these two effects, BOLD response in the presence of caffeine may either increase or decrease, likely the reason why earlier BOLD studies on caffeine often had seemingly contradictory results (101–104). Using simultaneous ASL and BOLD acquisitions to "calibrate" the BOLD response, Perthen and colleagues demonstrated that caffeine significantly alters CBF and cerebral oxygen consumption (CMRO2) coupling at rest, with a higher degree of intersubject variation when compared to visual stimulation (105). This result was extended by Chen and Parrish who used calibrated BOLD (106) to show that caffeine not only alters baseline hemodynamics, but also decreases CBF:CMRO2 coupling in both motor and visual tasks (107). The vasoconstrictive effects of caffeine also alter the temporal dynamics of the BOLD response (103,108), potentially due to the increased vascular tone of the constricted blood vessels. These studies highlight how ASL and BOLD can provide complementary information in the rapidly growing field of phMRI.

ASL MRI offers several advantages as a potential biomarker of drug actions. Firstly, ASL has been shown to have high reproducibility over periods of day, weeks, or months (109–111), making it suitable for studying oral drugs and chronic treatment. Its ability to quantify CBF, a biological parameter, means that it should also be suitable for multisite studies involving differing scanning platforms, though this capability has not yet been fully validated and dealing with current variations in ASL implementations across scanner platforms remains a challenge. Several recent studies have begun to demonstrate the utility of ASL MRI as a biomarker of pharmacological actions in the brain. Finally, ASL can be used to disentangle the complexity of the BOLD contrast. In fact, a few studies have used a combination of both techniques to provide complementary information about brain activity (105,107). As ASL continues to gain in popularity and availability, such combined studies are expected to become increasingly common. The use of ASL MRI to monitor the effects of pharmacological treatment for tobacco addiction is described in the following section.

Black et al. (112) employed a placebo-controlled, repeated-measure, crossover study design to investigate the mechanism of a novel adenosine A2A antagonist – SYN115 in 21 Parkinson Disease patients with levodopa infusion. Subjects were scanned with the commercial Siemens PASL sequence after a week of SYN115 treatment, taken twice a day. After a one week washout period, the experiment was repeated with a week's treatment of placebo. A subset of the subjects was assigned to 20mg (N=12) and 60mg (N=14) dose of SYN115 to facilitate quantification of a dose-response curve. In addition to a small decrease in global CBF (4% and 7% for 20mg and 60mg respectively), the authors reported significant decrease in thalamic CBF, consistent with the expected disinhibition of basal ganglia pathway by A_{2a} antagonists. This is also supported by earlier studies on treatment of Parkinsonian symptoms with A_{2a} antagonists. This study was one of the first that uses ASL to investigate mechanism of a novel drug, as well as provide a quantitative dose response curve.

Chen et al. (113) tested the feasibility of pseudocontinous ASL (pCASL) to detect the effect of a single, oral dose of citalopram on CBF. Twelve healthy subjects were randomized to receive either placebo or 20mg of citalopram, with a week's washout period between the two. Baseline pCASL scans were collected before drug intake, as well as 30 minutes, 1 hour and 3 hours post-medication. Using support vector machine (SVM), the authors reported significant drug-induced CBF decreases in regions including the amygdala, fusiform, insula and orbitofrontal cortex. Mixed effects analysis on CBF data extracted from selected regions of interest revealed a significant drug effect in the serotonergic regions. Combined with findings of elevated CBF in the same regions of depressed patients as well as subjects genetically prone to depression, these results suggest a potential mechanism for the clinical efficacy of citalopram in the treatment of depression.

Fernandez-Seara et al. (114) *also* demonstrated the feasibility of using ASL to detect single oral drug dose, in this case 10mg of metoclopramide or placebo was given to 18 healthy subjects. pCASL scans were acquired both before and one hour post-medication. To minimize variability due to inaccurate pCASL labeling efficiency, this study employed an additional phase-contrast scan to estimate the labeling efficiency in each subject (115) rather than using an assumed literature value. The authors reported bilateral increases in regional CBF in the putamen, globus pallidus and thalamus, as well as decreased regional CBF in bilateral insula, extending to the anterior temporal lobes. These results are consistent with findings in other antipsychotic drug studies using PET, and are further supported by pathological hyperperfusion in similar areas observed in Parkinson's disease patients.

Tolentino et al. (116) used PASL to investigate the effect of alcohol ingestion on CBF in a large number of subjects comprising of those at high and low risks for alcohol use disorders.

Eighty-eight young, healthy subjects were divided into matched pairs of high and low levels of response (LR) to alcohol, and assigned in randomized order to receive either 0.7–0.75ml/kg of ethanol or placebo (in the form of a non-caffeinated beverage). PASL scans were acquired 22 minutes after beverage ingestion. Consistent with earlier reports using other CBF measuring methodologies (PET, SPECT and ^{133}Xe inhalation), the authors observed CBF increases in the frontal regions. Additionally, this CBF increase was smaller in subjects with low LR to alcohol, which is also in agreement with earlier functional MRI studies.

ASL MRI in Neuropsychiatry

ASL MRI provides a versatile tool for quantifying regional brain function associated with "states", "traits", evoked responses, and pharmacological actions, all of which may be manifested by changes in regional CBF. These properties are particularly valuable in the investigation of neuropsychiatric disorders and their treatment. Initial studies have demonstrated the utility of ASL in several areas including tobacco addiction.

Franklin et al. (117) used the temporal stability of ASL MRI to compare brain function during smoking versus nonsmoking cues while controlling for withdrawal effects by having subjects smoke a cigarette before each measurement. CBF in preselected limbic regions including ventral striatum, amygdala, orbitofrontal cortex, hippocampus, medial thalamus, and left insula was higher during smoking versus nonsmoking cues, while cue-induced graving scores positively correlated with CBF changes in the dorsolateral prefrontal cortex and posterior cingulate. This pattern of activation was consistent with prior preclinical on the neural correlates of conditioned drug reward. In a subsequent report, the effects of dopamine transporter (DAT) polymorphisms on the observed effects were examined (118). Correlations between brain activity and craving were strong in one genotype subgroup and absent in the other, providing evidence that genetic variation in the DAT gene contributes to the neural and behavioral response variations elicited by smoking cues.

Three week's treatment with the smoking cessation medication varenicline was found to reduce cue induced craving as well as reactivity to smoking cues in reward-activating ventral striatum and medial orbitofrontal cortex (119). In the absence of smoking cues, varenicline treatment also increased CBF in reward-evaluating lateral orbitofrontal cortex, suggesting that varenicline may have dual effects that contribute to its efficacy.

A similar neural response was observed after three weeks of treatment with baclofen (120), which also decreased CBF in ventral striatum and medial orbitofrontal cortex (Figure 6) and increased CBF in lateral orbitofrontal cortex. Baclofen additionally diminished CBF in the insula, a region where infarction resulting in spontaneous smoking cessation.

A related study examined brain-behavior relationships in the absence of smoking cues. Wang et al. (121) studied a cohort of smokers under conditions of satiety and overnight abstinence. Smoking abstinence was associated with increased CBF anterior cingulate cortex, medial orbitofrontal cortex (Figure 6), and left OFC. Abstinence-induced cravings to smoke were predicted by CBF increases in the brain's visuospatial and reward circuitry, including in the right OFC, right dorsolateral prefrontal cortex, occipital cortex, ACC, ventral striatum/nucleus accumbens, thalamus, amygdala, bilateral hippocampus, left caudate, and right insula. This craving response was subsequently correlated with functional genetic variants previously associated with nicotine dependence (122). Significant modulations in the correlation between CBF and craving were observed with D2 receptor and catechol-o-methyl transferase genotype variations, suggesting a neural mechanism whereby these genetic variants may be linked with nicotine dependence.

ASL MRI has also begun to be applied to other neuropsychiatric syndromes. In affective disorders such as depression (123,124) and schizophrenia (125), hypoperfusion of prefrontal cortex has been observed and ASL MRI has been used in conjunction with other modalities to monitor treatment effects (126). Normalization of hyperperfusion in cortical and subcortical regions with stimulant therapy in a small cohort of patients with attention deficit hyperactivity disorder was also demonstrated using ASL MRI (127). Very recently, serial ASL MRI studies have been used to demonstrate objective neural correlates of post-surgical pain by performing imaging before and after dental extractions (128).

Summary

Over the past two decades ASL MRI has evolved from feasibility to practical utility and concomitant with the maturation of this technology, diverse applications of ASL MRI have also emerged. While most applications of ASL have been in basic and clinical neuroscience, ASL MRI can also be performed in other tissues, and applications outside of the brain are expected to emerge in the near future. ASL is nearly unique among MRI contrast mechanisms in that its biological basis, perfusion, is known. The ability to provide absolute quantification of a key biological parameter also makes it a very useful biomarker for both longitudinal and cross-sectional studies. CBF is a versatile biomarker of both normal and pathological brain function as illustrated by the findings summarized above, and inclusion of ASL in large cross-sectional and longitudinal databases will likely lead to valuable new insights into the neural basis for a wide range of behaviors and disorders. Use of ASL as a biomarker of drug actions and neural responses to therapy is also likely to contribute significantly to the development and validation of new therapies for brain disorders as well as disorders outside of the brain.

Given the utility of CBF measurement in clinical management, it is perplexing that ASL MRI has not really found its way into routine clinical practice. The explanation for this is likely multifactorial. Firstly, ASL MRI is based on weak signals, and ASL methodologies are somewhat more complex than other MRI methods in routine use. Secondly, the utility and benefits of ASL have been eclipsed by related technologies such as dynamic susceptibility contrast perfusion MRI and BOLD fMRI that are more widely available. Finally, clinicians are not accustomed to being able to quantify CBF easily, so do rarely demand it. Hopefully the availability and dissemination of truly robust ASL MRI implementations and a growing literature of applications demonstrating its utility will lead to its more widespread use for the betterment of both patient care and biomedical research.

Acknowledgments

Grant Support: NS058386, NS045839, RR002305, and MH080729

References

1. Ackerman JJ, Ewy CS, Becker NN, Shalwitz RA. Deuterium nuclear magnetic resonance measurements of blood flow and tissue perfusion employing 2H2O as a freely diffusible tracer. Proc Natl Acad Sci U S A. 1987; 84(12):4099–4102. [PubMed: 3035569]
2. Detre JA, Subramanian VH, Mitchell MD, et al. Measurement of regional cerebral blood flow in cat brain using intracarotid 2H2O and 2H NMR imaging. Magn Reson Med. 1990; 14(2):389–395. [PubMed: 2345518]
3. Eleff SM, Schnall MD, Ligetti L, et al. Concurrent measurement of cerebral blood flow, sodium, lactate, and high-energy phosphate metabolism using 19F, 23Na, 1H, and 31P nuclear magnetic resonance spectroscopy. Magn Reson Med. 1988; 7(4):412–424. [PubMed: 3173056]
4. Detre JA, Eskey CJ, Koretsky AP. Measurement of cerebral blood flow in rat brain using trifluoromethane and 19F-NMR. Magn Reson Med. 1990; 15(1):45–57. [PubMed: 2374499]

5. Detre JA, Leigh JS, Williams DS, Koretsky AP. Perfusion imaging. Magn Reson Med. 1992; 23(1): 37–45.
6. Ye FQ, Berman KF, Ellmore T, et al. H(2)(15)O PET validation of steady-state arterial spin tagging cerebral blood flow measurements in humans. Magn Reson Med. 2000; 44(3):450–456. [PubMed: 10975898]
7. Feng CM, Narayana S, Lancaster JL, et al. CBF changes during brain activation: fMRI vs. PET NeuroImage. 2004; 22(1):443–446.
8. Chen JJ, Wieckowska M, Meyer E, Pike GB. Cerebral blood flow measurement using fMRI and PET: a cross-validation study. International journal of biomedical imaging. 2008; 2008:516359. [PubMed: 18825270]
9. Alsop DC, Detre JA. Reduced transit-time sensitivity in noninvasive magnetic resonance imaging of human cerebral blood flow. J Cereb Blood Flow Metab. 1996; 16:1236–1249. [PubMed: 8898697]
10. Hendrikse J, Petersen ET, van Laar PJ, Golay X. Cerebral border zones between distal end branches of intracranial arteries: MR imaging. Radiology. 2008; 246(2):572–580. [PubMed: 18055872]
11. Zaharchuk G, Bammer R, Straka M, et al. Arterial spin-label imaging in patients with normal bolus perfusion-weighted MR imaging findings: pilot identification of the borderzone sign. Radiology. 2009; 252(3):797–807. [PubMed: 19703858]
12. MacIntosh BJ, Lindsay AC, Kylintireas I, et al. Multiple inflow pulsed arterial spin-labeling reveals delays in the arterial arrival time in minor stroke and transient ischemic attack. AJNR American journal of neuroradiology. 2010; 31(10):1892–1894. [PubMed: 20110375]
13. Bokkers RP, van der Worp HB, Mali WP, Hendrikse J. Noninvasive MR imaging of cerebral perfusion in patients with a carotid artery stenosis. Neurology. 2009; 73(11):869–875. [PubMed: 19752454]
14. Bokkers RP, van Laar PJ, van de Ven KC, Kapelle LJ, Klijn CJ, Hendrikse J. Arterial spin-labeling MR imaging measurements of timing parameters in patients with a carotid artery occlusion. AJNR American journal of neuroradiology. 2008; 29(9):1698–1703. [PubMed: 18701581]
15. Wu WC, St Lawrence KS, Licht DJ, Wang DJ. Quantification issues in arterial spin labeling perfusion magnetic resonance imaging. Topics in magnetic resonance imaging : TMRI. 2010; 21(2):65–73. [PubMed: 21613872]
16. Buxton RB, Frank LR, Wong EC, Siewert B, Warach S, Edelman RR. A general kinetic model for quantitative perfusion imaging with arterial spin labeling. Magn Reson Med. 1998; 40(3):383–396. [PubMed: 9727941]
17. Petersen ET, Lim T, Golay X. Model-free arterial spin labeling quantification approach for perfusion MRI. Magn Reson Med. 2006; 55(2):219–232. [PubMed: 16416430]
18. Wells JA, Thomas DL, King MD, Connelly A, Lythgoe MF, Calamante F. Reduction of errors in ASL cerebral perfusion and arterial transit time maps using image de-noising. Magn Reson Med. 2010; 64(3):715–724. [PubMed: 20578044]
19. Williams DS, Detre JA, Leigh JS, Koretsky AP. Magnetic resonance imaging of perfusion using spin inversion of arterial water. Proc Natl Acad Sci USA. 1992; 89(1):212–216. [PubMed: 1729691]
20. Edelman RR, Siewert B, Darby DG, et al. Qualitative mapping of cerebral blood flow and functional localization with echo-planar MR imaging and signal targeting with alternating radio frequency. Radiology. 1994; 192(2):513–520. [PubMed: 8029425]
21. Wong EC, Buxton RB, Frank LR. Quantitative imaging of perfusion using a single subtraction (QUIPSS and QUIPSS II). Magn Reson Med. 1998; 39(5):702–708. [PubMed: 9581600]
22. Kim SG. Quantification of relative cerebral blood flow change by flow-sensitive alternating inversion recovery (FAIR) technique: application to functional mapping. Magn Reson Med. 1995; 34(3):293–301. [PubMed: 7500865]
23. Wu WC, Fernandez-Seara M, Detre JA, Wehrli FW, Wang J. A theoretical and experimental investigation of the tagging efficiency of pseudocontinuous arterial spin labeling. Magn Reson Med. 2007; 58(5):1020–1027. [PubMed: 17969096]

24. Dai W, Garcia D, de Bazelaire C, Alsop DC. Continuous flow-driven inversion for arterial spin labeling using pulsed radio frequency and gradient fields. Magn Reson Med. 2008; 60(6):1488–1497. [PubMed: 19025913]
25. Davies NP, Jezzard P. Selective arterial spin labeling (SASL): perfusion territory mapping of selected feeding arteries tagged using two-dimensional radiofrequency pulses. Magn Reson Med. 2003; 49(6):1133–1142. [PubMed: 12768592]
26. Werner R, Norris DG, Alfke K, Mehdorn HM, Jansen O. Continuous artery-selective spin labeling (CASSL). Magn Reson Med. 2005; 53(5):1006–1012. [PubMed: 15844162]
27. Jones CE, Wolf RL, Detre JA, et al. Structural MRI of carotid artery atherosclerotic lesion burden and characterization of hemispheric cerebral blood flow before and after carotid endarterectomy. NMR Biomed. 2006; 19(2):198–208. [PubMed: 16475206]
28. van Osch MJ, Hendrikse J, Golay X, Bakker CJ, van der Grond J. Non-invasive visualization of collateral blood flow patterns of the circle of Willis by dynamic MR angiography. Med Image Anal. 2006; 10(1):59–70. [PubMed: 15950521]
29. Dai W, Robson PM, Shankaranarayanan A, Alsop DC. Modified pulsed continuous arterial spin labeling for labeling of a single artery. Magn Reson Med. 2010; 64(4):975–982. [PubMed: 20665896]
30. Wong EC. Vessel-encoded arterial spin-labeling using pseudocontinuous tagging. Magn Reson Med. 2007; 58(6):1086–1091. [PubMed: 17969084]
31. Duhamel G, de Bazelaire C, Alsop DC. Evaluation of systematic quantification errors in velocity-selective arterial spin labeling of the brain. Magn Reson Med. 2003; 50(1):145–153. [PubMed: 12815689]
32. Wong EC, Cronin M, Wu WC, Inglis B, Frank LR, Liu TT. Velocity-selective arterial spin labeling. Magn Reson Med. 2006; 55(6):1334–1341. [PubMed: 16700025]
33. Robson PM, Dai W, Shankaranarayanan A, Rofsky NM, Alsop DC. Time-resolved vessel-selective digital subtraction MR angiography of the cerebral vasculature with arterial spin labeling. Radiology. 2010; 257(2):507–515. [PubMed: 20959548]
34. Gunther M, Oshio K, Feinberg DA. Single-shot 3D imaging techniques improve arterial spin labeling perfusion measurements. Magn Reson Med. 2005; 54(2):491–498. [PubMed: 16032686]
35. Ye FQ, Frank JA, Weinberger DR, McLaughlin AC. Noise reduction in 3D perfusion imaging by attenuating the static signal in arterial spin tagging (ASSIST). Magn Reson Med. 2000; 44(1):92–100. [PubMed: 10893526]
36. Fernandez-Seara MA, Edlow BL, Hoang A, Wang J, Feinberg DA, Detre JA. Minimizing acquisition time of arterial spin labeling at 3T. Magn Reson Med. 2008; 59(6):1467–1471. [PubMed: 18506806]
37. Garcia DM, Duhamel G, Alsop DC. Efficiency of inversion pulses for background suppressed arterial spin labeling. Magn Reson Med. 2005; 54(2):366–372. [PubMed: 16032674]
38. Warach S, Dashe JF, Edelman RR. Clinical outcome in ischemic stroke predicted by early diffusion-weighted and perfusion magnetic resonance imaging; a preliminary analysis. J Cereb Blood Flow Metab. 1996; 16(1):53–59. [PubMed: 8530555]
39. Chalela JA, Alsop DC, Gonzalez-Atavalez JB, Maldjian JA, Kasner SE, Detre JA. Magnetic resonance perfusion imaging in acute ischemic stroke using continuous arterial spin labeling. Stroke. 2000; 31(3):680–687. [PubMed: 10700504]
40. Pollock JM, Deibler AR, Burdette JH, et al. Migraine associated cerebral hyperperfusion with arterial spin-labeled MR imaging. AJNR Am J Neuroradiol. 2008; 29(8):1494–1497. [PubMed: 18499796]
41. Pollock JM, Deibler AR, West TG, Burdette JH, Kraft RA, Maldjian JA. Arterial spin-labeled magnetic resonance imaging in hyperperfused seizure focus: a case report. J Comput Assist Tomogr. 2008; 32(2):291–292. [PubMed: 18379320]
42. Detre JA, Samuels OB, Alsop DC, Gonzalez-At JB, Kasner SE, Raps EC. Noninvasive MRI evaluation of CBF with acetazolamide challenge in patients with cerebrovascular stenosis. JMRI. 1999; 10:870–875. [PubMed: 10548801]

43. Ances BM, McGarvey ML, Abrahams JM, et al. Continuous arterial spin labeled perfusion magnetic resonance imaging in patients before and after carotid endarterectomy. J Neuroimaging. 2004; 14(2):133–138. [PubMed: 15095558]
44. Jefferson AL, Glosser G, Detre JA, Sinson G, Liebeskind DS. Neuropsychological and perfusion MR imaging correlates of revascularization in a case of moyamoya syndrome. AJNR Am J Neuroradiol. 2006; 27(1):98–100. [PubMed: 16418365]
45. Hendrikse J, van Osch MJ, Rutgers DR, et al. Internal carotid artery occlusion assessed at pulsed arterial spin-labeling perfusion MR imaging at multiple delay times. Radiology. 2004; 233(3): 899–904. [PubMed: 15486211]
46. Chng SM, Petersen ET, Zimine I, Sitoh YY, Lim CC, Golay X. Territorial arterial spin labeling in the assessment of collateral circulation: comparison with digital subtraction angiography. Stroke; a journal of cerebral circulation. 2008; 39(12):3248–3254.
47. Wolf RL, Wang J, Detre JA, Zager EL, Hurst RW. Arteriovenous shunt visualization in arteriovenous malformations with arterial spin-labeling MR imaging. AJNR Am J Neuroradiol. 2008; 29(4):681–687. [PubMed: 18397967]
48. Oguz KK, Golay X, Pizzini FB, et al. Sickle cell disease: continuous arterial spin-labeling perfusion MR imaging in children. Radiology. 2003; 227(2):567–574. [PubMed: 12663827]
49. Chen J, Licht DJ, Smith SE, et al. Arterial spin labeling perfusion MRI in pediatric arterial ischemic stroke: initial experiences. J Magn Reson Imaging. 2009; 29(2):282–290. [PubMed: 19161176]
50. Licht DJ, Wang J, Silvestre DW, et al. Preoperative cerebral blood flow is diminished in neonates with severe congenital heart defects. J Thorac Cardiovasc Surg. 2004; 128(6):841–849. [PubMed: 15573068]
51. Wu WC, Mohler E 3rd, Ratcliffe SJ, Wehrli FW, Detre JA, Floyd TF. Skeletal muscle microvascular flow in progressive peripheral artery disease: assessment with continuous arterial spin-labeling perfusion magnetic resonance imaging. J Am Coll Cardiol. 2009; 53(25):2372–2377. [PubMed: 19539149]
52. Wang DJ, Bi X, Avants BB, Meng T, Zuehlsdorff S, Detre JA. Estimation of perfusion and arterial transit time in myocardium using free-breathing myocardial arterial spin labeling with navigator-echo. Magn Reson Med. 2010; 64(5):1289–1295. [PubMed: 20865753]
53. Roberts DA, Detre JA, Bolinger L, et al. Renal perfusion in humans: MR imaging with spin tagging of arterial water. Radiology. 1995; 196(1):281–286. [PubMed: 7784582]
54. Maleki N, Dai W, Alsop DC. Blood flow quantification of the human retina with MRI. NMR Biomed. 2011; 24(1):104–111. [PubMed: 20862658]
55. Wolf RL, Wang J, Wang S, et al. Grading of CNS neoplasms using continuous arterial spin labeled perfusion MR imaging at 3 Tesla. J Magn Reson Imaging. 2005; 22(4):475–482. [PubMed: 16161080]
56. Noguchi T, Yoshiura T, Hiwatashi A, et al. Perfusion imaging of brain tumors using arterial spin-labeling: correlation with histopathologic vascular density. AJNR Am J Neuroradiol. 2008; 29(4): 688–693. [PubMed: 18184842]
57. Ozsunar Y, Mullins ME, Kwong K, et al. Glioma recurrence versus radiation necrosis? A pilot comparison of arterial spin-labeled, dynamic susceptibility contrast enhanced MRI, and FDG-PET imaging. Acad Radiol. 2010; 17(3):282–290. [PubMed: 20060750]
58. de Bazelaire C, Alsop DC, George D, et al. Magnetic resonance imaging-measured blood flow change after antiangiogenic therapy with PTK787/ZK 222584 correlates with clinical outcome in metastatic renal cell carcinoma. Clin Cancer Res. 2008; 14(17):5548–5554. [PubMed: 18765547]
59. Alsop DC, Detre JA, Grossman M. Assessment of cerebral blood flow in Alzheimer's disease by spin-labeled magnetic resonance imaging. Ann Neurol. 2000; 47(1):93–100. [PubMed: 10632106]
60. Johnson NA, Jahng GH, Weiner MW, et al. Pattern of cerebral hypoperfusion in Alzheimer disease and mild cognitive impairment measured with arterial spin-labeling MR imaging: initial experience. Radiology. 2005; 234(3):851–859. [PubMed: 15734937]
61. Du AT, Jahng GH, Hayasaka S, et al. Hypoperfusion in frontotemporal dementia and Alzheimer disease by arterial spin labeling MRI. Neurology. 2006; 67(7):1215–1220. [PubMed: 17030755]

62. Alsop DC, Dai W, Grossman M, Detre JA. Arterial Spin Labeling Blood Flow MRI: Its Role in the Early Characterization of Alzheimer's Disease. J Alzheimers Dis. 2010; 20(3):871–880. [PubMed: 20413865]
63. Hu WT, Wang Z, Lee VM, Trojanowski JQ, Detre JA, Grossman M. Distinct cerebral perfusion patterns in FTLD and AD. Neurology. 2010; 75(10):881–888. [PubMed: 20819999]
64. Chao LL, Buckley ST, Kornak J, et al. ASL perfusion MRI predicts cognitive decline and conversion from MCI to dementia. Alzheimer Dis Assoc Disord. 2010; 24(1):19–27. [PubMed: 20220321]
65. Wolf RL, Alsop DC, Levy-Reis I, et al. Detection of mesial temporal lobe hypoperfusion in patients with temporal lobe epilepsy by use of arterial spin labeled perfusion MR imaging. AJNR Am J Neuroradiol. 2001; 22(7):1334–1341. [PubMed: 11498422]
66. Lim YM, Cho YW, Shamim S, et al. Usefulness of pulsed arterial spin labeling MR imaging in mesial temporal lobe epilepsy. Epilepsy Res. 2008; 82(2–3):183–189. [PubMed: 19041041]
67. Pendse N, Wissmeyer M, Altrichter S, et al. Interictal arterial spin-labeling MRI perfusion in intractable epilepsy. J Neuroradiol. 2010; 37(1):60–63. [PubMed: 19674791]
68. Detre JA, Alsop DC. Perfusion MRI with continuous arterial spin labeling: Methods and clinical applications in the nervous system. Eur J Radiol. 1999; 30(2):115–124. [PubMed: 10401592]
69. Davis TL, Kwong KK, Weisskoff RM, Rosen BR. Calibrated functional MRI: Mapping the dynamics of oxydative metabolism. Proc Natl Acad Sci USA. 1998; 95(4):1834–1839. [PubMed: 9465103]
70. Wang J, Licht DJ, Jahng GH, et al. Pediatric perfusion imaging using pulsed arterial spin labeling. J Magn Reson Imaging. 2003; 18(4):404–413. [PubMed: 14508776]
71. Chiron C, Raynaud C, Maziere B, et al. Changes in regional cerebral blood flow during brain maturation in children and adolescents. J Nucl Med. 1992; 33(5):696–703. [PubMed: 1569478]
72. Miranda MJ, Olofsson K, Sidaros K. Noninvasive measurements of regional cerebral perfusion in preterm and term neonates by magnetic resonance arterial spin labeling. Pediatr Res. 2006; 60(3): 359–363. [PubMed: 16857776]
73. Biagi L, Abbruzzese A, Bianchi MC, Alsop DC, Del Guerra A, Tosetti M. Age dependence of cerebral perfusion assessed by magnetic resonance continuous arterial spin labeling. Journal of magnetic resonance imaging : JMRI. 2007; 25(4):696–702. [PubMed: 17279531]
74. Wang, J.; Rao, H.; Detre, JA. Arterial spin labeling perfusion MRI in developmental neuroscience. In: Rumsey, JM.; Ernst, M., editors. Neuroimging in Developmental Clinical Neuroscience. Cambridge: Cambridge University Press; 2009. p. 326-343.
75. Taki Y, Hashizume H, Sassa Y, et al. Correlation between gray matter density-adjusted brain perfusion and age using brain MR images of 202 healthy children. Hum Brain Mapp. 201110.1002/hbm.21163
76. Gogtay N, Giedd JN, Lusk L, et al. Dynamic mapping of human cortical development during childhood through early adulthood. Proc Natl Acad Sci U S A. 2004; 101(21):8174–8179. [PubMed: 15148381]
77. Chugani HT, Phelps ME. Maturational changes in cerebral function in infants determined by 18FDG positron emission tomography. Science. 1986; 231(4740):840–843. [PubMed: 3945811]
78. Wang Z, Fernandez-Seara M, Alsop DC, et al. Assessment of functional development in normal infant brain using arterial spin labeled perfusion MRI. NeuroImage. 2008; 39(3):973–978. [PubMed: 17988892]
79. Duong TQ, Silva AC, Lee SP, Kim SG. Functional MRI of calcium-dependent synaptic activity: cross correlation with CBF and BOLD measurements. Magn Reson Med. 2000; 43(3):383–392. [PubMed: 10725881]
80. Silva AC, Lee SP, Iadecola C, Kim SG. Early temporal characteristics of cerebral blood flow and deoxyhemoglobin changes during somatosensory stimulation. J Cereb Blood Flow Metab. 2000; 20(1):201–206. [PubMed: 10616809]
81. Huppert TJ, Hoge RD, Diamond SG, Franceschini MA, Boas DA. A temporal comparison of BOLD, ASL, and NIRS hemodynamic responses to motor stimuli in adult humans. NeuroImage. 2006; 29(2):368–382. [PubMed: 16303317]

82. Zarahn E, Aguirre GK, D'Esposito M. Empirical analyses of BOLD fMRI statistics: I. Spatially unsmoothed data collected under null-hypothesis conditions. NeuroImage. 1997; 5(3):179–197. [PubMed: 9345548]
83. Aguirre GK, Detre JA, Alsop DC. Experimental design and the relative sensitivity of BOLD and perfusion fMRI. NeuroImage. 2002; 15(3):488–500. [PubMed: 11848692]
84. Wang J, Aguirre GK, Kimberg DY, Roc AC, Li L, Detre JA. Arterial spin labeling perfusion fMRI with very low task frequency. Magn Reson Med. 2003; 49(5):796–802. [PubMed: 12704760]
85. Olson IR, Rao H, Moore KS, Wang J, Detre JA, Aguirre GK. Using perfusion fMRI to measure continuous changes in neural activity with learning. Brain Cogn. 2006; 60(3):262–271. [PubMed: 16423439]
86. Wang J, Rao H, Wetmore GS, et al. Perfusion functional MRI reveals cerebral blood flow pattern under psychological stress. Proc Natl Acad Sci U S A. 2005; 102(49):17804–17809. [PubMed: 16306271]
87. Wang J, Korczykowski M, Rao H, et al. Gender Difference in Neural Response to Psychological Stress. Soc Cogn Affect Neurosci. 2007; 2(3):227–239. [PubMed: 17873968]
88. Lim J, Wu WC, Wang J, Detre JA, Dinges DF, Rao H. Imaging brain fatigue from sustained mental workload: an ASL perfusion study of the time-on-task effect. NeuroImage. 2010; 49(4): 3426–3435. [PubMed: 19925871]
89. Gillihan SJ, Rao H, Wang J, et al. Serotonin transporter genotype modulates amygdala activity during mood regulation. Social cognitive and affective neuroscience. 2010; 5(1):1–10. [PubMed: 19858108]
90. Wang DJ, Rao H, Korczykowski M, et al. Cerebral blood flow changes associated with different meditation practices and perceived depth of meditation. Psychiatry research. 2011; 191:60–67. [PubMed: 21145215]
91. Rao H, Wang J, Tang K, Pan W, Detre JA. Imaging brain activity during natural vision using CASL perfusion fMRI. Hum Brain Mapp. 2007; 28(7):593–601. [PubMed: 17034034]
92. Raichle ME. Neuroscience. The brain's dark energy. Science. 2006; 314(5803):1249–1250. [PubMed: 17124311]
93. Hermes M, Hagemann D, Britz P, et al. Latent state-trait structure of cerebral blood flow in a resting state. Biol Psychol. 2009; 80(2):196–202. [PubMed: 18838099]
94. Rao H, Gillihan SJ, Wang J, et al. Genetic variation in serotonin transporter alters resting brain function in healthy individuals. Biol Psychiatry. 2007; 62(6):600–606. [PubMed: 17481593]
95. Gillihan SJ, Rao H, Brennan L, et al. Serotonin transporter genotype modulates the association between depressive symptoms and amygdala activity among psychiatrically healthy adults. Psychiatry research. 2011
96. Canli T, Qiu M, Omura K, et al. Neural correlates of epigenesis. Proc Natl Acad Sci U S A. 2006; 103(43):16033–16038. [PubMed: 17032778]
97. Abler B, Hofer C, Viviani R. Habitual emotion regulation strategies and baseline brain perfusion. Neuroreport. 2008; 19(1):21–24. [PubMed: 18281886]
98. Beschoner P, Richter S, Lo H, et al. Baseline brain perfusion and working memory capacity: a neuroimaging study. Neuroreport. 2008; 19(18):1803–1807. [PubMed: 18978646]
99. Gianaros PJ, Sheu LK, Remo AM, Christie IC, Crtichley HD, Wang J. Heightened resting neural activity predicts exaggerated stressor-evoked blood pressure reactivity. Hypertension. 2009; 53(5): 819–825. [PubMed: 19273741]
100. Ashburner J, Friston KJ. Voxel-based morphometry--the methods. NeuroImage. 2000; 11(6 Pt 1): 805–821. [PubMed: 10860804]
101. Laurienti PJ, Field AS, Burdette JH, Maldjian JA, Yen YF, Moody DM. Dietary caffeine consumption modulates fMRI measures. NeuroImage. 2002; 17(2):751–757. [PubMed: 12377150]
102. Mulderink TA, Gitelman DR, Mesulam MM, Parrish TB. On the use of caffeine as a contrast booster for BOLD fMRI studies. NeuroImage. 2002; 15(1):37–44. [PubMed: 11771972]
103. Liu TT, Behzadi Y, Restom K, et al. Caffeine alters the temporal dynamics of the visual BOLD response. NeuroImage. 2004; 23(4):1402–1413. [PubMed: 15589104]

104. Koppelstaetter F, Poeppel TD, Siedentopf CM, et al. Does caffeine modulate verbal working memory processes? An fMRI study. NeuroImage. 2008; 39(1):492–499. [PubMed: 17936643]

105. Perthen JE, Lansing AE, Liau J, Liu TT, Buxton RB. Caffeine-induced uncoupling of cerebral blood flow and oxygen metabolism: a calibrated BOLD fMRI study. NeuroImage. 2008; 40(1): 237–247. [PubMed: 18191583]

106. Chen Y, Parrish TB. Caffeine's effects on cerebrovascular reactivity and coupling between cerebral blood flow and oxygen metabolism. NeuroImage. 2009; 44(3):647–652. [PubMed: 19000770]

107. Chen Y, Parrish TB. Caffeine dose effect on activation-induced BOLD and CBF responses. NeuroImage. 2009; 46(3):577–583. [PubMed: 19289172]

108. Liau J, Perthen JE, Liu TT. Caffeine reduces the activation extent and contrast-to-noise ratio of the functional cerebral blood flow response but not the BOLD response. NeuroImage. 2008; 42(1):296–305. [PubMed: 18514545]

109. Chen Y, Wang DJ, Detre JA. Test-retest reliability of arterial spin labeling with common labeling strategies. Journal of magnetic resonance imaging : JMRI. 2011; 33(4):940–949. [PubMed: 21448961]

110. Gevers S, Majoie CB, van den Tweel XW, Lavini C, Nederveen AJ. Acquisition time and reproducibility of continuous arterial spin-labeling perfusion imaging at 3T. AJNR American journal of neuroradiology. 2009; 30(5):968–971. [PubMed: 19193760]

111. Petersen ET, Mouridsen K, Golay X. The QUASAR reproducibility study, Part II: Results from a multi-center Arterial Spin Labeling test-retest study. NeuroImage. 2010; 49(1):104–113. [PubMed: 19660557]

112. Black KJ, Koller JM, Campbell MC, Gusnard DA, Bandak SI. Quantification of indirect pathway inhibition by the adenosine A2a antagonist SYN115 in Parkinson disease. J Neurosci. 2010; 30(48):16284–16292. [PubMed: 21123574]

113. Chen Y, Wan HI, O'Reardon JP, et al. Quantification of cerebral blood flow as biomarker of drug effect: arterial spin labeling phMRI after a single dose of oral citalopram. Clin Pharmacol Ther. 2011; 89(2):251–258. [PubMed: 21191380]

114. Fernandez-Seara MA, Aznarez-Sanado M, Mengual E, Irigoyen J, Heukamp F, Pastor MA. Effects on resting cerebral blood flow and functional connectivity induced by metoclopramide: a perfusion MRI study in healthy volunteers. Br J Pharmacol. 201010.1111/j.1476-5381.2010.01161.x

115. Aslan S, Xu F, Wang PL, et al. Estimation of labeling efficiency in pseudocontinuous arterial spin labeling. Magnetic resonance in medicine : official journal of the Society of Magnetic Resonance in Medicine/Society of Magnetic Resonance in Medicine. 2010; 63(3):765–771. [PubMed: 20187183]

116. Tolentino NJ, Wierenga CE, Hall S, et al. Alcohol Effects on Cerebral Blood Flow in Subjects With Low and High Responses to Alcohol. Alcohol Clin Exp Res. 201110.1111/j.1530-0277.2011.01435.x

117. Franklin TR, Wang Z, Wang J, et al. Limbic activation to cigarette smoking cues independent of nicotine withdrawal: a perfusion fMRI study. Neuropsychopharmacology. 2007; 32(11):2301–2309. [PubMed: 17375140]

118. Franklin TR, Lohoff FW, Wang Z, et al. DAT genotype modulates brain and behavioral responses elicited by cigarette cues. Neuropsychopharmacology. 2009; 34(3):717–728. [PubMed: 18704100]

119. Franklin T, Wang Z, Suh JJ, et al. Effects of varenicline on smoking cue-triggered neural and craving responses. Archives of general psychiatry. 2011; 68(5):516–526. [PubMed: 21199958]

120. Franklin TR, Wang Z, Sciortino N, et al. Modulation of resting brain cerebral blood flow by the GABA B agonist, baclofen: A longitudinal perfusion fMRI study. Drug and alcohol dependence. 2011

121. Wang Z, Faith M, Patterson F, et al. Neural substrates of abstinence-induced cigarette cravings in chronic smokers. J Neurosci. 2007; 27(51):14035–14040. [PubMed: 18094242]

122. Wang Z, Ray R, Faith M, et al. Nicotine abstinence-induced cerebral blood flow changes by genotype. Neurosci Lett. 2008; 438(3):275–280. [PubMed: 18499348]

123. Duhameau B, Ferre JC, Jannin P, et al. Chronic and treatment-resistant depression: a study using arterial spin labeling perfusion MRI at 3Tesla. Psychiatry research. 2010; 182(2):111–116. [PubMed: 20427157]

124. Lui S, Parkes LM, Huang X, et al. Depressive disorders: focally altered cerebral perfusion measured with arterial spin-labeling MR imaging. Radiology. 2009; 251(2):476–484. [PubMed: 19401575]

125. Scheef L, Manka C, Daamen M, et al. Resting-state perfusion in nonmedicated schizophrenic patients: a continuous arterial spin-labeling 3. 0-T MR study. Radiology. 2010; 256(1):253–260. [PubMed: 20505069]

126. Freudenmann RW, Kolle M, Huwe A, et al. Delusional infestation: neural correlates and antipsychotic therapy investigated by multimodal neuroimaging. Prog Neuropsychopharmacol Biol Psychiatry. 2010; 34(7):1215–1222. [PubMed: 20600460]

127. O'Gorman RL, Mehta MA, Asherson P, et al. Increased cerebral perfusion in adult attention deficit hyperactivity disorder is normalised by stimulant treatment: a non-invasive MRI pilot study. NeuroImage. 2008; 42(1):36–41. [PubMed: 18511306]

128. Howard MA, Krause K, Khawaja N, et al. Beyond patient reported pain: perfusion magnetic resonance imaging demonstrates reproducible cerebral representation of ongoing post-surgical pain. PloS one. 2011; 6(2):e17096. [PubMed: 21373203]

129. Franklin TR, Wang Z, Sciortino N, et al. Modulation of resting brain cerebral blood flow by the GABA B agonist, baclofen: A longitudinal perfusion fMRI study. Drug Alcohol Depend. 201110.1016/j.drugalcdep.2011.01.015

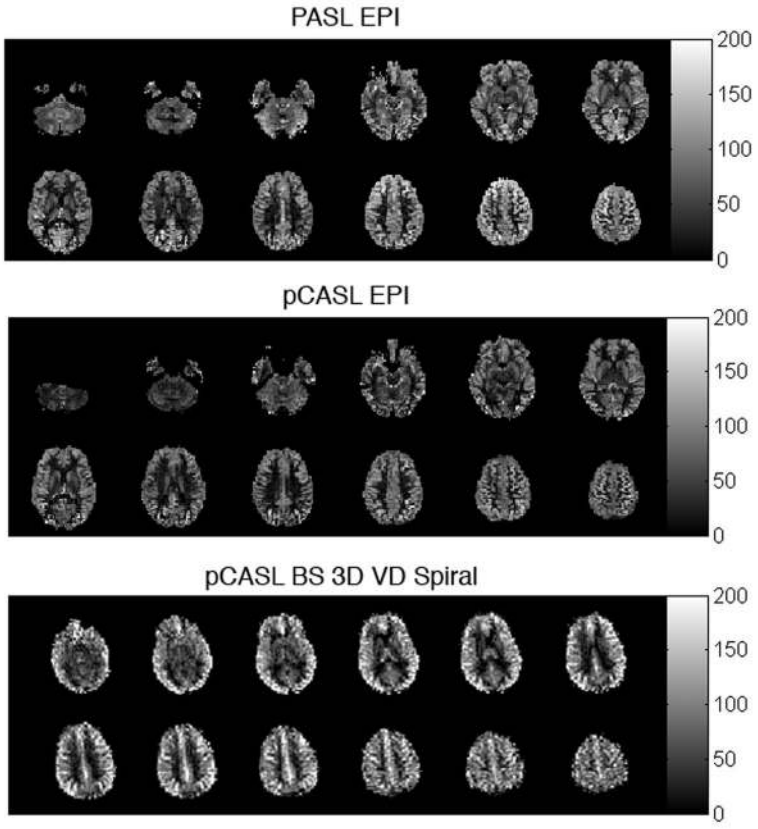

Figure 1.
Typical whole-brain ASL MRI quantitative CBF data obtained in 6 minutes at 3 Tesla using PASL and pCASL with echoplanar imaging (TOP and MIDDLE), adapted from (109) with permission from the publisher. BELOW: pCASL with background-suppressed 3-dimensional variable density spiral acquisition acquired in 2 minutes at 3 Tesla.

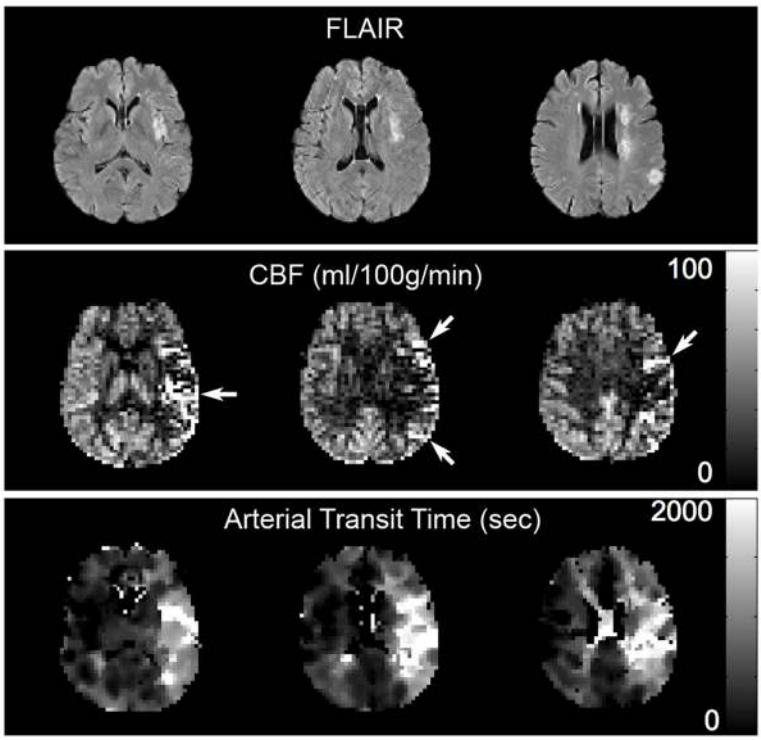

Figure 2.
Transit artifact in a patient with left middle cerebral artery stroke and a transit time map showing prolonged arterial transit to this region. TOP: FLAIR images showing multiple strokes in the left MCA distribution. MIDDLE: ASL CBF images show artifactual hyperperfusion in the left MCA distribution (arrows) due to delayed transit of label, which is imaged within leptomenigeal vessels providing collateral flow. CBF in left and right MCA distributions are actually nearly identical at 43 and 42 ml/100g/min, respectively. Bottom: Arterial transit time map demonstrates prolonged transit times to the left MCA distribution.

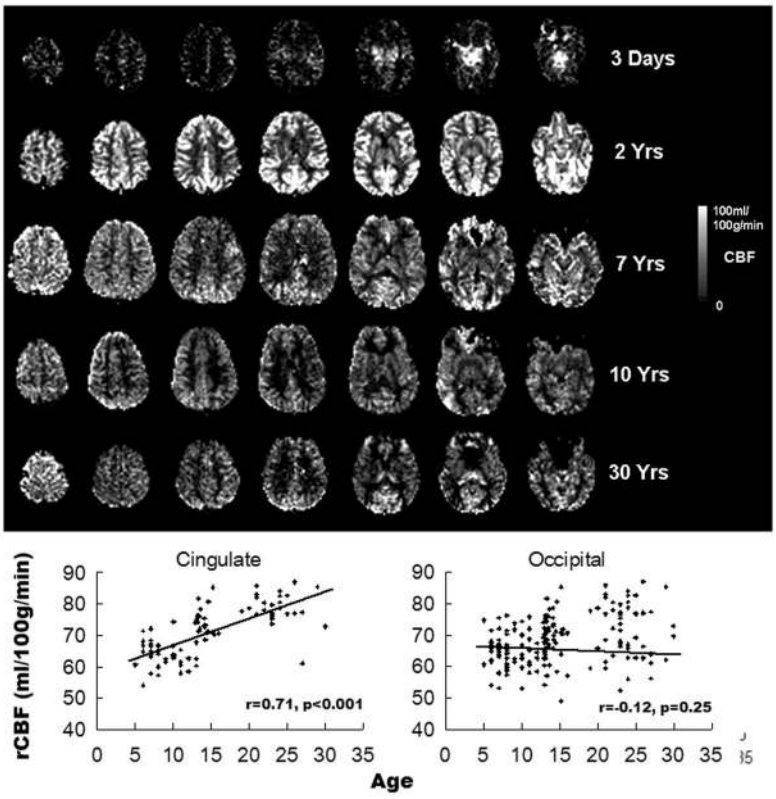

Figure 3.

TOP: Representative ASL MRI data across human brain development. BELOW: ROI data showing developmental trajectories of relative CBF in cingulate and occipital cortices. An increase in cingulate CBF is evident, while occipital CBF remains stable.

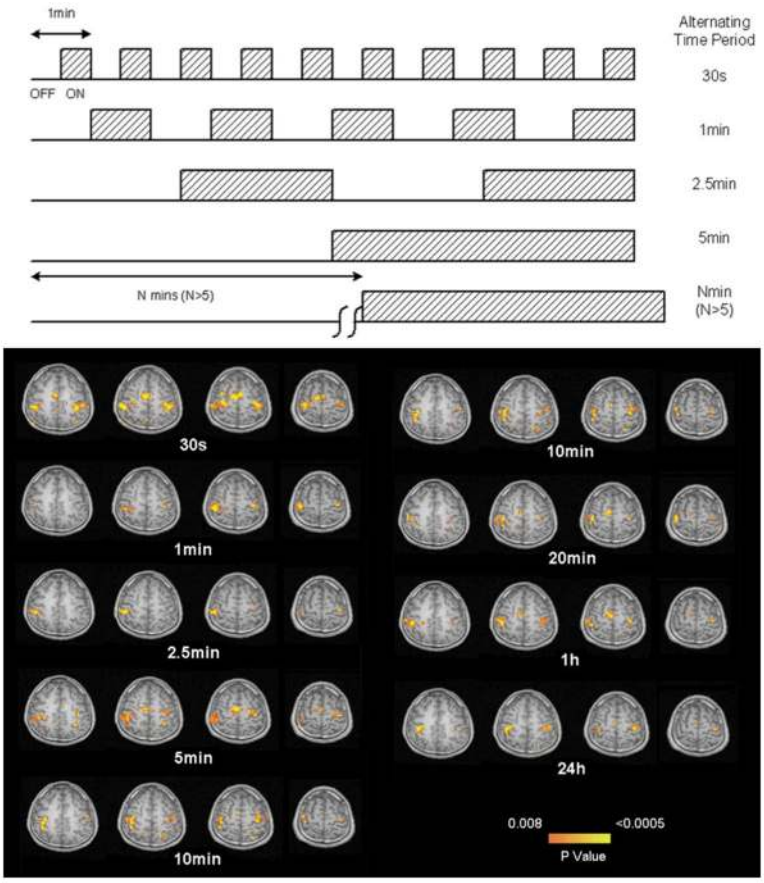

Figure 4.
Temporal stability of ASL perfusion fMRI. Successful demonstration of motor cortex activation with bilateral finger tapping is observed even when task and activation are carried out on successive days, 24 hours apart. The experimental design is shown above. Adapted from (84) with permission from the publisher.

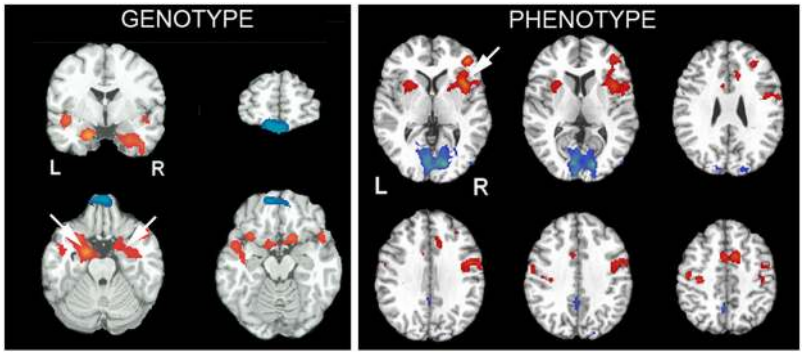

Figure 5.
Demonstration of genotype and phenotype effects in resting ASL MRI data. LEFT: increased perfusion of amygdala in patients with a serotonin transporter genotype that confers an increased risk of depression and anxiety. RIGHT: Resting perfusion in right medial frontal cortex predicts subsequent time-on-task fatiguability. Adapted from (88,94) with permission from the publisher.

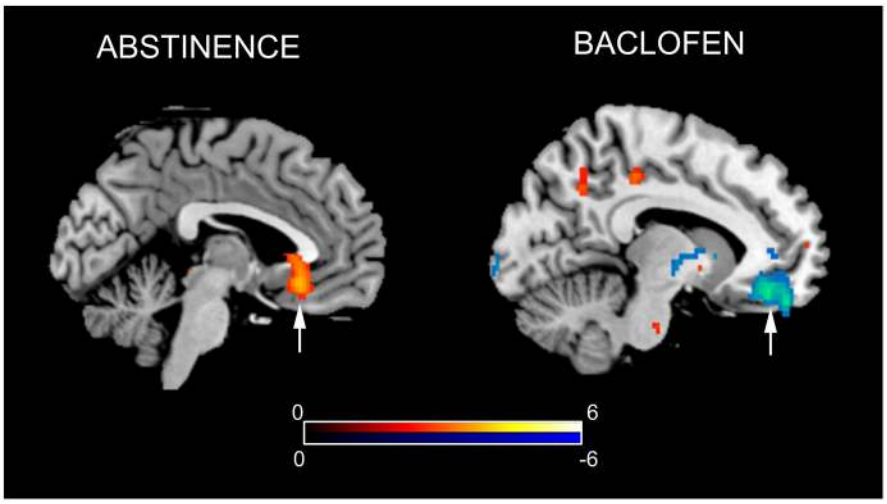

Figure 6.
Increase in orbitofrontal cortex CBF after overnight abstinence in smokers (LEFT) and reduction in CBF in this region after treatment with baclofen (RIGHT). Adapted from (121,129) with permission from the publisher.